Controlling the behavior of single live cells with high density arrays of microscopic OLEDs

*Anja Steude, Matthias Jahnel, Michael Thomschke, Matthias Schober and Malte C. Gather**

Dr. A. Steude, Prof. M. C. Gather
SUPA, School of Physics and Astronomy, University of St Andrews, North Haugh, St Andrews, KY16 9SS, United Kingdom, phone: +44-1334-46-3108
E-mail: mcg6@st-andrews.ac.uk

M.Sc. M. Jahnel, Dr. M. Thomschke, Dr. M. Schober
Fraunhofer Institut für Elektronenstrahl und Plasmatechnik und COMEDD (FEP)
Maria-Reiche-Str. 2, 01109 Dresden, Germany

Keywords: organic light-emitting diodes; optogenetics; micro-display; thin-film encapsulation; biophotonics

Since their invention by Tang and Van Slyke in 1987[1], organic light-emitting diodes (OLEDs) have matured into highly efficient and versatile light sources. By today they have secured a substantial share of the market for mobile phone displays and are prime candidates for a range of applications including large area displays, luminescent signage and large lighting panels for glare-free solid-state illumination.[2–5] The organic conjugated molecules on which OLEDs are based offer nearly unlimited possibilities for chemical tuning of their characteristics, such as color of emission[6], and enable light-weight devices with inherent mechanical flexibility[7–9]. Compared to conventional inorganic LEDs, OLEDs are based on less toxic materials and their production has significantly lower environmental impact. OLEDs achieve sub-µs switching and their excellent efficiency allows high brightness levels without excessive heat production. Integration with suitable backplane driver electronics enables spatially controlled generation of light as required for high-resolution displays. These features also render the technology attractive for applications in biotechnology and biomedicine where controlled illumination is crucial, e.g. in optogenetics – a technique that enables precise control of neuronal behavior with light[10,11]. However, device encapsulation represents a major challenge in this context, because contact with biological material typically

involves immersion into water/salt solutions and exposing OLEDs to even a few mg of water per m² of device area leads to catastrophic device failure[12]. So far OLEDs have therefore been applied primarily in enclosed light sources[13] and photonic sensors[14–18].

Here, we capitalize on the above characteristics of the OLED technology and, in addition, show how OLEDs can be brought into close contact (< 2 µm) with an aqueous environment containing live cells. Our thin-film encapsulated micro-arrays comprising several hundred thousand µm-sized OLEDs provide the spatial control required for lens-free illumination of individual live cells and for controlling their behavior in real time. The OLED arrays used here were originally developed as microdisplays for electronic viewfinders and video glasses but in this study we show that they can be modified – in particular in terms of emission spectrum and encapsulation – to become a novel biophotonics platform for structured illumination with exquisite spatial and temporal control. To illustrate the potential of this concept, we investigated the light-controlled locomotion (phototaxis) of the green alga *Chlamydomonas reinhardtii*, a famous model organism for cellular movement and light-sensing[19]. *C. reinhardtii* is also the natural source of Channelrhodopsin 1 and 2 (ChR1/2), the genetically encoded photoreceptors used in optogenetics[10,11]. Our work thus paves the way for using bio-integrated OLED array light sources to control and study neuronal activity and cell signaling.

Figure 1a shows a picture and a schematic illustration of the OLED micro-arrays used in this study. The arrays consisted of 320 x 720 individual fluorescent blue top-emitting OLEDs with p-i-n architecture, each measuring 6 µm x 9 µm. To achieve independent control of the brightness of each OLED, the organic layer stack forming the OLED was deposited on a silicon-based CMOS backplane which is connected to external control electronics through a flexible flat cable. Figure 1b shows a microscope image of an operating OLED array,

displaying the logo of the University of St Andrews. The pattern shown by the array can be updated at video rate (up to 120 Hz), thus allowing the illumination pattern to be changed at high frame rates (see Supporting Information, **Video 1**).

To address the issue of encapsulation, the OLEDs used in this study were protected by a ~1.3 µm thick multilayer thin-film encapsulation consisting of alternating layers of aluminum oxide and a cross-linked acrylic polymer (see Figure 1a). The layer sequence, 3 x Al_2O_3 and 2 x Barix™ polymer, complies with typical encapsulation standards for micro-displays. The encapsulating effect of multilayer structures is well described in literature and low water vapor transmission rates of 10^{-5} - 10^{-6} $gm^{-2}day^{-1}$are reached by this technique.[20–22]
No additional glass encapsulation was applied as this would prohibit lens-free illumination of individual cells with high-resolution light patterns due to the divergence of the light emitted by the OLEDs.

To establish the effectiveness of the thin film encapsulation, the active area of OLED arrays was immersed in deionized water or physiological salt buffer solution for 72 h. The brightness at a fixed current and the voltage required to achieve a pre-set current were measured before and after the immersion test. The changes due to the incubation were less than the sample-to-sample variation and not statistically significant (Figure 1c), indicating that the encapsulation should be suited for a wide range of in vitro and possibly in vivo experiments.

The light sensitivity of most photosensitive compounds found in biology is strongly wavelength-dependent and many show highest sensitivity in the blue part of the spectrum. The action spectra of the photoreceptors ChR1 and ChR2, present in *C. reinhardtii*, peak at 480 nm[23] and 470 nm[24], respectively (Figure 1d). The OLEDs used in this study were

designed to provide an emission spectrum that closely matches the spectral response of ChR1 and ChR2 (Figure 1d, peak wavelength, 477 nm; full-width-at-half-maximum, 44 nm).

Figure 2a shows a microscope image of the *C. reinhardtii* alga we used to evaluate the ability of our OLED arrays to control cell behavior. Each alga cell possesses two flagella —lash-like attachments extending from the cell body— which it uses to swim in a breast-stroke like manner. During movement, the cell body rotates counter clockwise around the axis of forward motion. *C. reinhardtii* sense modulations of light and change the direction of movement accordingly to optimize conditions for photosynthesis[19]. This is achieved by the directional sensitivity of the orange eye spot, a light sensing structure at the cell equator that is formed by stacked layers of lipid vesicles containing high refractive index carotenoids and by ChR1/ChR2 localized within the cell membrane (Figure 2b). The eye spot is most sensitive to light incident perpendicular to its surface because the multi-layer carotenoid structure forms a natural Bragg reflector which concentrates incident light onto the region of the cell membrane where the channelrhodopsins are located. It is believed that activation of channelrhodopsins by blue light triggers a cascade of events inducing a change of the resting cell membrane potential and a calcium influx at the flagella membrane[23–25]. This increase in intracellular calcium concentration affects how strongly one flagella moves compared to the other which changes the direction in which the cell moves. As the cell continuously turns around its axis in a helical motion, the change in flagella dominance allows the alga to move towards a light source.

We investigated the phototactic behavior of two algae strains, *CC*-125 and *CC*-2894, upon exposure to different optical stimuli from the OLED micro-array; in particular, with respect to cell accumulation, cell speed and directionality. *CC*-125 is phototactic whereas *CC*-2894 is known to exhibit negligible phototaxis[26]. A cell suspension was applied to the OLED arrays

and cell aggregation for both strains was monitored for different brightness levels. Figure 2c shows microscope images of the blue emission from an OLED micro-array and of the cell aggregation for *CC*-125 after 0 min and 2 min of OLED illumination with 1.1 W m^{-2} of blue light. Analyzing the change in cell density as a function of optical power density reveals distinct differences in the phototactic behavior between the two cell strains (Figure 2d). The density of *CC*-125 on the illuminated patch of the array increased with optical power at a rate of ~4200 cells per (W m^{-2}), consistent with positive phototaxis. By contrast, the density of *CC*-2894 cells did not change across the whole range of optical power densities applied, providing further evidence that the movement of *CC*-125 cells towards the operating OLEDs was a light-induced change in locomotion.

OLED illumination can also be used to study cell behavior in real-time. To illustrate this, we moved a square of active pixels across an OLED array loaded with *CC*-125 cells. Within seconds, cells adjusted their swimming direction to the active OLEDs (Figure 2e; Supporting Information, **Video 2**). Such dynamic studies of phototaxis at the microscopic level would be difficult to realize with a similar level of flexibility when using an external macroscopic light source.

Besides studying the collective cell behavior, we investigated in real time the influence of light on individual cells. We monitored the movement of *CC*-125 and *CC*-2894 cells under OLED illumination at different brightness levels (see Supporting Information, **Video 3**). For each strain and optical intensity, the position of 10 algae cells was tracked for 2 s (immediately after the cells first entered the illuminated area). **Figure 3a** shows tracks for cells from both strains recorded at 0.025 W m^{-2} and 1.1 W m^{-2}, respectively. At low optical power, *CC*-125 cells moved in straight lines across the illuminated area but at higher intensity cells frequently changed direction and remained trapped on top of the active OLEDs. By

contrast, the tracks of the *CC*-2894 control cells resembled the low-intensity behavior of the *CC*-125 regardless of OLED brightness. To better understand the differences in movement, we analyzed the tracking data further. The mean straight line speed (Figure 3b) and the mean modulus of the turning angle (Figure 3c) of the non-phototactic *CC*-2894 control cells were relatively stable over the whole range of optical power densities applied. By contrast, for the light sensitive *CC*-125 cells the straight line speed decreased and the mean modulus of their turning angle increased significantly over the range of OLED brightness tested indicating that these cells changed their direction of motion in response to light exposure to keep moving towards the light source.

In summary, we demonstrated for the first time that OLED micro-arrays can be used for lens-free, optical near-field, microscopic manipulation of live cells. We were able to investigate modifications in speed and swimming direction of *Chlamydomonas rheinhardtii* due to light stimulation. Our OLED arrays are ideal platforms to e.g. investigate the influence of light on propulsive forces on the cell body and the flagellum[27,28] which would increase the understanding of phototaxis. Our study is particularly relevant to neurobiology because photoreceptors isolated from the model organism we used in our work are frequently employed as optogenetic tools to obtain light-mediated control over neuronal cells. OLED micro-arrays offer a set of unique properties not shared by other technologies: Compared to the conventional LED micro-arrays, the OLEDs achieve higher pixel density and larger total number of pixels. By chemical tuning the emission spectrum of OLEDs can be tailored to various light-sensitive targets. Due to their stable, ultra-thin encapsulation, our OLED micro-arrays achieve high resolution structured illumination without any of the projection optics typically required for laser scanning or spatial light modulator based approaches. Future OLED devices can be flexible, bio-implantable and potentially biodegradable. By using stacked devices with two separately controlled OLEDs of different color, co-located target

molecules with different activity spectra may be addressed individually.[29,30] Our work thus paves the way for accurate light-activated control of a variety of biological systems.

Experimental Section

***OLED micro-arrays*:** OLED micro-arrays were based on a CMOS backplane with an active area of about 20 mm^2 and 230,000 individually addressable pixels, each defined by a 6 x 9 µm² sized aluminum anode. CMOS wafers comprising 667 individual chips were coated with a blue-emitting fluorescent *p-i-n* OLED stack (Novaled, Germany) using thermal evaporation under high vacuum (base pressure, 10^{-7} mbar). At an initial brightness of 1000 cd m^{-2} the operational lifetime of the OLED stack is 15000 h. A common cathode (thickness, < 15 nm) for all pixels on a chip was formed by a semi-transparent silver layer. A spacer layer of organic small molecules was deposited on top of the cathode by thermal evaporation to reduce tension and protect the OLED during the subsequent deposition of the encapsulation. The encapsulation consisted of alternating layers of 3 x Al2O3 (deposited by DC reactive sputtering) and 2 x Barix polymer (vacuum deposited as monomer precursor and cured by UV light) and was deposited in a system by Vitex Systems, USA (process described in [20]). To prevent damage during the subsequent wafer dicing step, a fluorinated resist (OSCOR 4000; Orthogonal, USA; thickness, 1.5 µm) was spun onto the wafer and cured for 1 min at 90°C. The wafer was laminated onto a dicing tape and after sawing, the resist was stripped off with Stripper 700 (Orthogonal, USA). Single chips were bonded onto a flexible flat cable that connects to a custom HDMI driver interface. The arrays were operated at a frame rate of 60 Hz or 120 Hz. Different brightness levels were set by changing the grey scale value of the input video signal. The optical power density was measured with a calibrated power meter (Gentec EO, Canada). The emission spectrum was recorded with a CCD spectrograph (Andor, UK). An epoxy ring around the edge of the OLED arrays retained the applied cell suspensions.

***Stability tests*:** The active area of the OLED arrays was covered with distilled water or physiological phosphate buffer (PBS pH 7.4; Life technologies, UK) and incubated with these solutions at 37°C for 72 h. Before and after incubation, the device luminance and current-voltage characteristics were measured on a Wentworth Pegasus S200 probe station. The luminance was measured at a pixel current of 8 nA with an Ocean Optics spectrometer USB4000 while a source measurement unit (SMU; Keithley 2400) drove the CMOS. Luminance was integrated over the active area. The voltage was measured passively by applying 1 mA from the SMU directly to the active area.

***Induction of phototaxis in C. reinhardtii with the OLED micro-arrays*:** Algae strains *CC*-125 and *CC*-2894 were obtained from the Chlamydomonas Resource Center (University of Minnesota, St. Paul, USA). They were cultured in standard Sueoka`s high salt medium.[31] Cultures were shaken at 215 rpm on a rotary shaker with illumination from a 60 W daylight bulb. Temperature was kept at 26°C. For phototaxis experiments, cell suspensions in growth medium were applied onto OLED micro-arrays (volume, 50 µL; cell count, 2.5 - 5 million per mL). For the cell aggregation test, images of the cells were taken with an upright microscope (Nikon Eclipse Ni-U) and a CMOS color camera (Net NS4133CU); illumination was provided with red light (> 600 nm, using long-pass filters) to avoid light-induced artefacts. Time lapse images were taken with the same microscope using an EMCCD camera (Andor) and a long-pass filter for NIR illumination (> 800 nm). Cell tracking experiments were performed with an inverted microscope (Nikon Ti-S). To trigger phototaxis, pixels of the micro-array were selectively switched by supplying an appropriate video signal to the HDMI controller.

***Image analysis*:** Time lapse images were analyzed using Fiji software[32] with the plugin MTrackJ[33].

Acknowledgements

This work was supported in part by the Scottish Funding Council (via SUPA) and the Human Frontier Science Program (HFSP). The authors thank Andrew Morton (U St Andrews) for fruitful discussions.

[1] C. W. Tang, S. A. VanSlyke, *Appl. Phys. Lett.* **1987**, *51*, 913.
[2] G. Gelinck, P. Heremans, K. Nomoto, T. D. Anthopoulos, *Adv. Mater.* **2010**, *22*, 3778.
[3] M. A. McCarthy, B. Liu, E. P. Donoghue, I. Kravchenko, D. Y. Kim, F. So, A. G. Rinzler, *Science* **2011**, *332*, 570.
[4] K. T. Kamtekar, A. P. Monkman, M. R. Bryce, *Adv. Mater.* **2010**, *22*, 572.
[5] M. C. Gather, A. Köhnen, K. Meerholz, *Adv. Mater.* **2011**, *23*, 233.
[6] L. Xiao, Z. Chen, B. Qu, J. Luo, S. Kong, Q. Gong, J. Kido, *Adv. Mater.* **2011**, *23*, 926.
[7] D. Zhang, K. Ryu, X. Liu, E. Polikarpov, J. Ly, M. E. Tompson, C. Zhou, *Nano Lett.* **2006**, *6*, 1880.
[8] Z. B. Wang, M. G. Helander, J. Qiu, D. P. Puzzo, M. T. Greiner, Z. M. Hudson, S. Wang, Z. W. Liu, Z. H. Lu, *Nat. Photonics* **2011**, *5*, 753.
[9] T.-H. Han, Y. Lee, M.-R. Choi, S.-H. Woo, S.-H. Bae, B. H. Hong, J.-H. Ahn, T.-W. Lee, *Nat. Photonics* **2012**, *6*, 105.
[10] G. Miller, *Science* **2006**, *314*, 1674.
[11] L. Fenno, O. Yizhar, K. Deisseroth, *Annu. Rev. Neurosci.* **2011**, *34*, 389.
[12] J.-S. Park, H. Chae, H. K. Chung, S. I. Lee, *Semicond. Sci. Technol.* **2011**, *26*, 034001.
[13] S. K. Attili, A. Lesar, A. McNeill, M. Camacho-Lopez, H. Moseley, S. Ibbotson, I. Samuel, J. Ferguson, *Br. J. Dermatol.* **2009**, *161*, 170.
[14] C. Wang, D. Hwang, Z. Yu, K. Takei, J. Park, T. Chen, B. Ma, A. Javey, *Nat. Mater.* **2013**, *12*, 899.
[15] F. Lefèvre, A. Chalifour, L. Yu, V. Chodavarapu, P. Juneau, R. Izquierdo, *Lab Chip* **2012**, *12*, 787.
[16] E. L. Ratcliff, P. A. Veneman, A. Simmonds, B. Zacher, D. Huebner, S. S. Saavedra, N. R. Armstrong, *Anal. Chem.* **2010**, *82*, 2734.
[17] S. Vengasandra, Y. Cai, D. Grewell, J. Shinar, R. Shinar, *Lab Chip* **2010**, *10*, 1051.
[18] M. C. Gather, N. M. Kronenberg, K. Meerholz, *Adv. Mater.* **2010**, *22*, 4634.
[19] K. Schaller, R. David, R. Uhl, *Biophys. J.* **1997**, *73*, 1562.
[20] L. Moro, D. Boesch, X. Zeng, in *OLED fundamentals: Materials, devices, and processing of organic light-emitting diodes* (Eds.: D. J. Gaspar, E. Polikarpov), CRC Press. Boca Raton, FLa., USA **2015**, pp. 25-66.
[21] L. L. Moro, T. A. Krajewski, N. M. Rutherford, O. Philips, R. J. Visser, M. E. Gross, W. D. Bennett, G. L. Graff, *Proc. SPIE* **2004**, *5214*.
[22] J. Park, Y.-Y. Noh, J. W. Huh, J. Lee, H. Chu, *Org. Electron.* **2012**, *13*, 1956.
[23] P. Berthold, S. P. Tsunoda, O. P. Ernst, W. Mages, D. Gradmann, P. Hegemann, *Plant Cell* **2008**, *20*, 1665.
[24] G. Nagel, T. Szellas, W. Huhn, S. Kateriya, N. Adeishvili, P. Berthold, D. Ollig, P. Hegemann, E. Bamberg, *Proc. Natl. Acad. Sci. U. S. A.* **2011**, *100*, 13940.
[25] K. W. Foster, R. D. Smyth, *Microbiol. Rev.* **1980**, *44*, 572.
[26] N. Okita, N. Isogai, M. Hirono, R. Kamiya, K. Yoshimura, *J. Cell Sci.* **2005**, *118*, 529.
[27] P. V. Bayly, B. L. Lewis, E. C. Ranz, R. J. Okamoto, R. B. Pless, S. K. Dutcher, *Biophys. J.* **2011**, *100*, 2716.
[28] I. Minoura, R. Kamiya, *Cell Motil. Cytoskeleton* **1995**, *31*, 130.

[29] Z. Shen, P. E. Burrows, V. Bulović, S. R. Forrest, M. E. Thompson, *Science* **1997**, *276*, 2009.
[30] M. Fröbel, T. Schwab, M. Kliem, S. Hofmann, K. Leo, M. C. Gather, *Light: Sci. Appl.* **2015**, *4*, e247.
[31] N. Sueoka, *Proc. Natl. Acad. Sci. U. S. A.* **1960**, *46*, 83.
[32] J. Schindelin, I. Arganda-Carreras, E. Frise, V. Kaynig, M. Longair, T. Pietzsch, S. Preibisch, C. Rueden, S. Saalfeld, B. Schmid, J.-Y. Tinevez, D. J. White, V. Hartenstein, K. Eliceiri, P. Tomancak, A. Cardona, *Nat. Methods* **2012**, *9*, 676.
[33] E. Meijering, O. Dzyubachyk, I. Smal, *Methods Enzymol.* **2012**, *504*, 183.

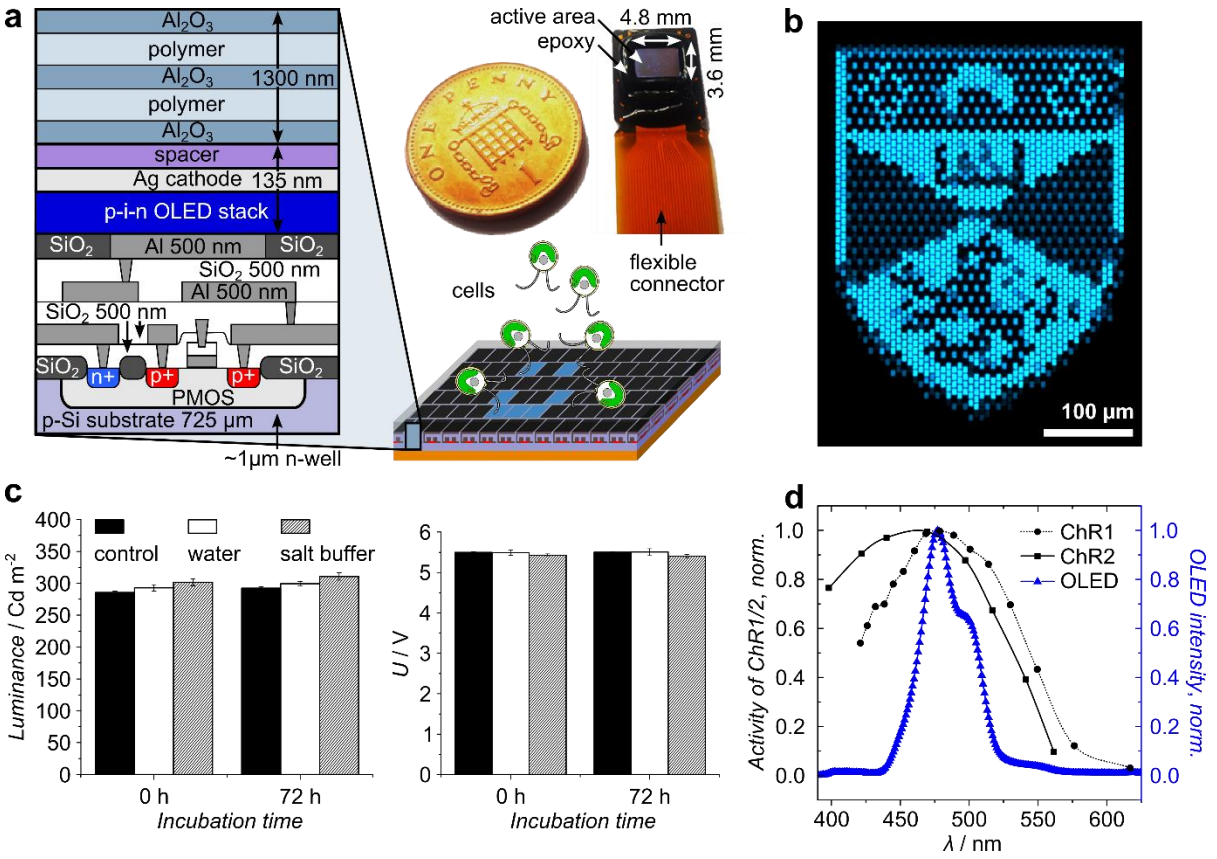

Figure 1. OLED micro-arrays for manipulation of cells with light: experimental setup, optical characteristics and stability of the OLEDs. a) Cross-section (left), schematic illustration (bottom right) and picture (top right) of OLED micro-arrays (not to scale). Arrays consist of ~2 × 10^5 blue top-emitting *p-i-n* OLEDs deposited on a CMOS backplane and protected by multi-layer thin film encapsulation. Cells are applied directly on top of the array and each pixel can be turned on and off to achieve controlled light exposure of individual cells. **b)** Microscopy image of a section of the display with pixel pattern adjusted to show the logo of the University of St Andrews. Each pixel is 6 µm x 9 µm in size. **c)** OLED luminance at 8 nA pixel current and voltage at a total display current of 1 mA measured before (0 h) and after incubation with water and salt buffer for 72 h (mean values of three or more micro-arrays with standard error of the mean as error bars). Control arrays were left untreated. **d)** Left axis: Activity spectrum of channelrhodopsin 1 (ChR1, circles)[23] and channelrhodopsin 2 (ChR2, squares)[24]. Right axis: Emission spectrum of blue OLED micro-array with multi-layer thin film encapsulation (blue triangles).

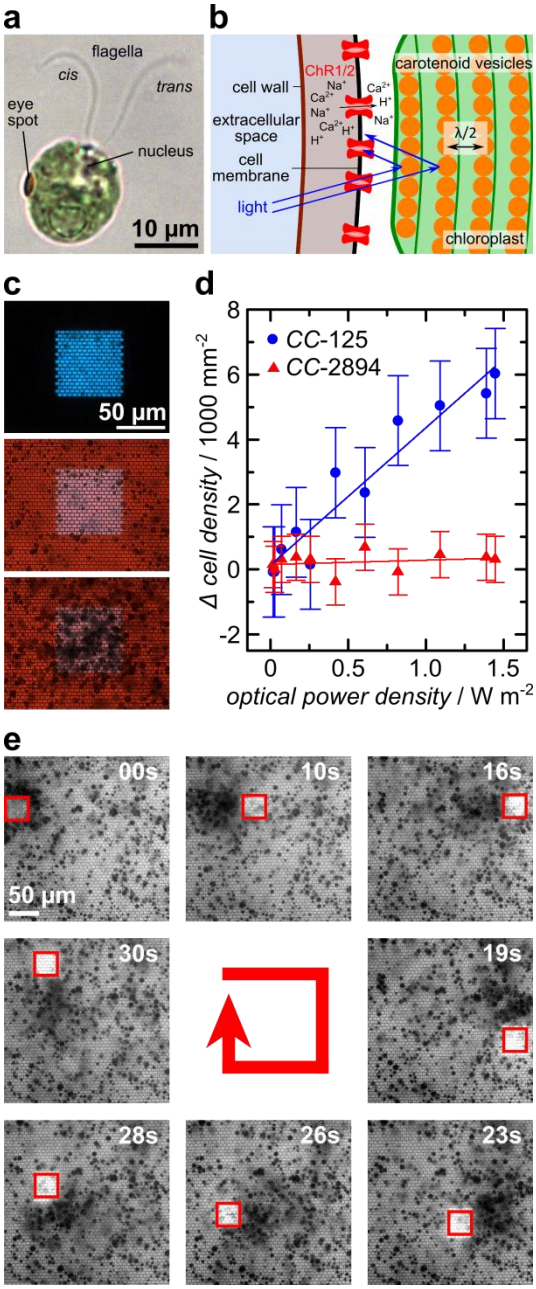

Figure 2. Phototaxis of the *CC*-125 and *CC*-2894 strains of *Chlamydomonas reinhardtii* induced with blue light generated by an OLED micro-array. a) Bright field microscopic image of a *CC*-125 cell with the two flagella (cis and trans relative to the eye spot) and the eye spot at the cell equator, **b)** Schematic of the eye spot (not to scale) composed of layers of carotenoid vesicles acting as light reflector and the photoreceptors Channelrhodopsin 1 and 2 (ChR1/2) in the cell membrane. **c)** Images of OLED array emission (top) and of *CC*-125 cells accumulating on top of the operated pixels of the array immediately after the pixels are tuned on (center, 0 min) and after 2 min of operation (bottom). Optical power density provided by OLED, 1.1 W m^{-2}. **d)** Change in cell density after 2 min of OLED operation versus optical power density of active pixels. Solid lines are linear fits to the data (error bars, standard deviation of initial cell number for each strain). **e)** Time lapse images of *CC*-125 cells following a square of OLED pixels for 30 s. Red squares indicate the pixels that are turned on.

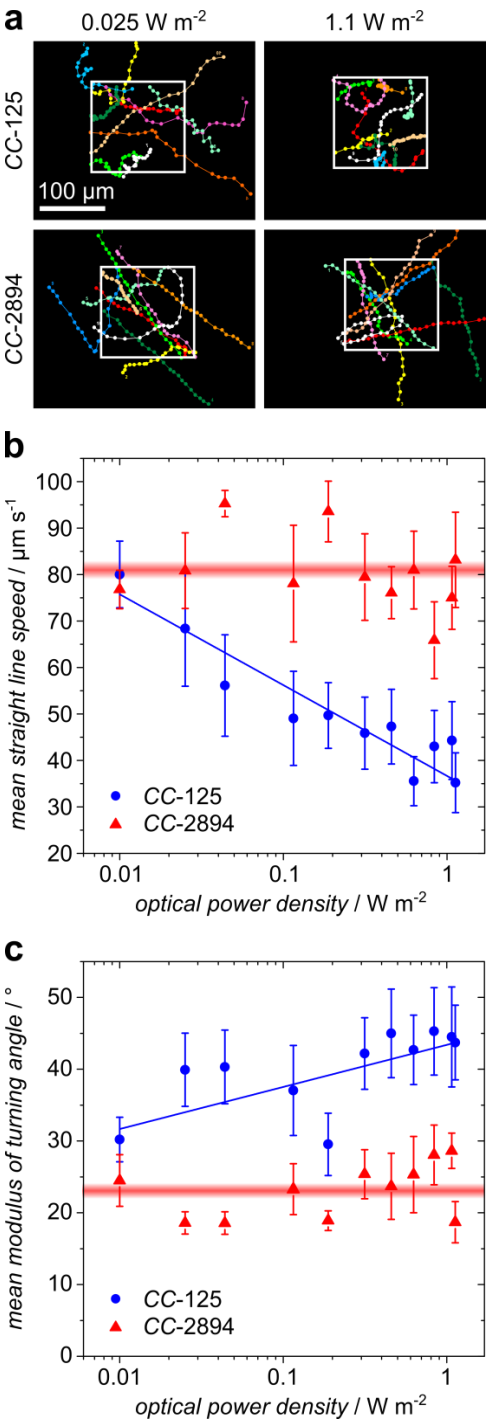

Figure 3. Using OLED micro-arrays to study the phototactic response of *Chlamydomonas reinhardtii* on single cell level. a) Trajectories of ten *CC*-125 and ten *CC*-2894 cells (each marked by different color circles) recorded over 2 s at 0.025 W m^{-2} and 1.1 W m^{-2} intensity, respectively. White squares indicate the 140 µm x 140 µm area of active OLED pixels. **b)** Mean straight line speed of the cells as a function of optical power density delivered by the micro-array for *CC*-125 (blue circle) and *CC*-2894 (red triangle, control). **c)** Mean modulus of turning angle of cells as a function of optical power density for *CC*-125 (blue circle) and *CC*-2894 (red triangle) cells. The red shaded areas in **b)** and **c)** indicate mean ± the standard error over the entire power range for the *CC*-2894 control cells. The solid blue lines are linear fits to the data for *CC*-125.